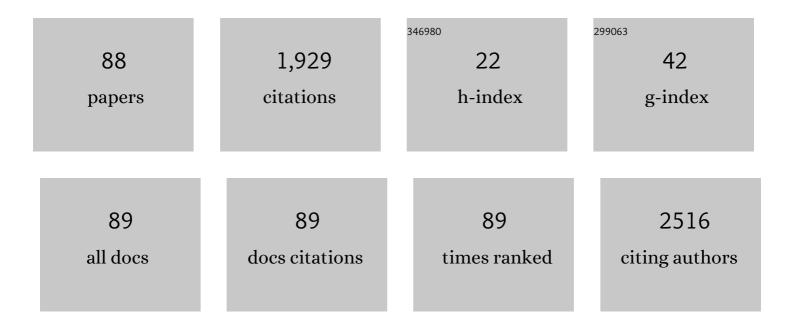
Andrew L Goertzen

List of Publications by Year in descending order

Source: https://exaly.com/author-pdf/4331568/publications.pdf Version: 2024-02-01



#	Article	IF	CITATIONS
1	A Cube-Based Dual-GPU List-Mode Reconstruction Algorithm for PET Imaging. IEEE Transactions on Radiation and Plasma Medical Sciences, 2022, 6, 463-474.	2.7	1
2	Prediction of 2-year major adverse cardiac events from myocardial perfusion scintigraphy and clinical risk factors. Journal of Nuclear Cardiology, 2022, 29, 1956-1963.	1.4	6
3	Age-related reduction of hemispheric asymmetry by pigeons: A behavioral and FDG-PET imaging investigation of visual discrimination. Learning and Behavior, 2022, 50, 125-139.	0.5	2
4	Imaging Cerebral Glucose Metabolism during Dualâ€Task Walking in Patients with Parkinson's disease. Journal of Neuroimaging, 2021, 31, 356-362.	1.0	4
5	Changes in Metabolic Activity and Gait Function by Dual-Task Cognitive Game-Based Treadmill System in Parkinson's Disease: Protocol of a Randomized Controlled Trial. Frontiers in Aging Neuroscience, 2021, 13, 680270.	1.7	5
6	Alzheimer's Disease-Related Metabolic Pattern in Diverse Forms of Neurodegenerative Diseases. Diagnostics, 2021, 11, 2023.	1.3	9
7	CRAX: A simple cardiovascular risk assessment tool to predict risk of acute myocardial infarction or death. Journal of Nuclear Cardiology, 2020, 27, 2365-2374.	1.4	8
8	Geometry Optimization of a Dual-Layer Offset Detector for Use in Simultaneous PET/MR Neuroimaging. IEEE Transactions on Radiation and Plasma Medical Sciences, 2019, 3, 275-284.	2.7	9
9	Performance Characterization of MPPC Modules for TOF-PET Applications. IEEE Transactions on Radiation and Plasma Medical Sciences, 2019, 3, 475-482.	2.7	13
10	Count rate performance of brain-dedicated PET scanners: a Monte Carlo simulation study. Physics in Medicine and Biology, 2019, 64, 215013.	1.6	1
11	Fracture Risk Indices From DXA-Based Finite Element Analysis Predict Incident Fractures Independently From FRAX: The Manitoba BMD Registry. Journal of Clinical Densitometry, 2019, 22, 338-345.	0.5	15
12	Regional hypometabolism in the 3xTg mouse model of Alzheimer's disease. Neurobiology of Disease, 2019, 127, 264-277.	2.1	36
13	Towards a second-generation PET/MR insert with enhanced timing and count rate performance. Physics in Medicine and Biology, 2019, 64, 085017.	1.6	5
14	A study of inter-crystal scatter in dual-layer offset scintillator arrays for brain-dedicated PET scanners. Physics in Medicine and Biology, 2019, 64, 115007.	1.6	6
15	Blood Flow and Glucose Metabolism Dissociation in the Putamen Is Predictive of Levodopa Induced Dyskinesia in Parkinson's Disease Patients. Frontiers in Neurology, 2019, 10, 1217.	1.1	10
16	Comparison of acrylic polymer adhesive tapes and silicone optical grease in light sharing detectors for positron emission tomography. Physics in Medicine and Biology, 2018, 63, 05NT02.	1.6	3
17	Comparison of femoral strength and fracture risk index derived from DXA-based finite element analysis for stratifying hip fracture risk: A cross-sectional study. Bone, 2018, 110, 386-391.	1.4	11
18	Performance of a PET Insert for High-Resolution Small-Animal PET/MRI at 7 Tesla. Journal of Nuclear Medicine, 2018, 59, 536-542.	2.8	49

Andrew L Goertzen

#	Article	IF	CITATIONS
19	A phoswich detector design for improved spatial sampling in PET. Nuclear Instruments and Methods in Physics Research, Section A: Accelerators, Spectrometers, Detectors and Associated Equipment, 2018, 882, 124-128.	0.7	3
20	Machine learning identified an Alzheimer's disease-related FDG-PET pattern which is also expressed in Lewy body dementia and Parkinson's disease dementia. Scientific Reports, 2018, 8, 13236.	1.6	52
21	Distinct brain metabolic patterns separately associated with cognition, motor function, and aging in Parkinson's disease dementia. Neurobiology of Aging, 2017, 60, 81-91.	1.5	24
22	Long-Term Proton Pump Inhibitor Use Is Not Associated With Changes in Bone Strength and Structure. American Journal of Gastroenterology, 2017, 112, 95-101.	0.2	62
23	Data Acquisition for a Preclinical MR Compatible PET Insert Using the OpenPET Platform. IEEE Transactions on Radiation and Plasma Medical Sciences, 2017, 1, 495-504.	2.7	3
24	A prospective cohort study to assess the role of FDG-PET in differentiating benign and malignant follicular neoplasms. Annals of Medicine and Surgery, 2016, 12, 27-31.	0.5	12
25	An algorithm for automatic crystal identification in pixelated scintillation detectors using thin plate splines and Gaussian mixture models. Physics in Medicine and Biology, 2016, 61, N90-N101.	1.6	9
26	Geometry optimization of dual-layer offset detectors for compact ring diameter PET systems. , 2016, , .		4
27	First Results From a High-Resolution Small Animal SiPM PET Insert for PET/MR Imaging at 7T. IEEE Transactions on Nuclear Science, 2016, 63, 2424-2433.	1.2	45
28	Characterization of a Small Animal PET Detector Block Incorporating a Digital Photon Counter Array. IEEE Transactions on Nuclear Science, 2015, 62, 732-739.	1.2	4
29	Development of a PET Scanner for Simultaneously Imaging Small Animals with MRI and PET. Sensors, 2014, 14, 14654-14671.	2.1	21
30	Dual-Modality Preclinical PET/CT Instrumentation. , 2014, , 367-386.		0
31	Pixelated Geiger-Mode Avalanche Photo-Diode Characterization Through Dark Current Measurement. IEEE Transactions on Nuclear Science, 2014, 61, 1369-1375.	1.2	4
32	Optical Simulation of Dual-Ended Readout of Axially-Oriented 100 mm Long LYSO Crystals for Use in a Compact PET System. IEEE Transactions on Nuclear Science, 2014, 61, 3-13.	1.2	0
33	Multiplexing Approaches for a 12 x 4 Array of Silicon Photomultipliers. IEEE Transactions on Nuclear Science, 2014, 61, 35-43.	1.2	23
34	Evaluation of SiPM photodetectors for use in phoswich detectors. , 2014, , .		1
35	Maximization of Digital Photon Counter efficiency when using Neighbor Logic. , 2014, , .		0
36	Evaluation of performance and stability of an MR compatible PET detector. , 2014, , .		2

ANDREW L GOERTZEN

#	Article	IF	CITATIONS
37	Design and Performance of a Resistor Multiplexing Readout Circuit for a SiPM Detector. IEEE Transactions on Nuclear Science, 2013, 60, 1541-1549.	1.2	87
38	Characterization of a New MR Compatible Small Animal PET Scanner Using Monte-Carlo Simulations. IEEE Transactions on Nuclear Science, 2013, 60, 1637-1644.	1.2	18
39	Assessment of three techniques for delivering stem cells to the heart using PET and MR imaging. EJNMMI Research, 2013, 3, 72.	1.1	29
40	Simulation studies of a phoswich PET detector design with a two-fold improvement in spatial sampling. , 2013, , .		1
41	Comparison of single and dual layer detector blocks for pre-clinical MRI–PET. Nuclear Instruments and Methods in Physics Research, Section A: Accelerators, Spectrometers, Detectors and Associated Equipment, 2013, 702, 56-58.	0.7	18
42	A PET detector interface board and slow control system based on the Raspberry Pi [®] . , 2013, , .		6
43	Improved event positioning in a gamma ray detector using an iterative position-weighted centre-of-gravity algorithm. Physics in Medicine and Biology, 2013, 58, N189-N200.	1.6	14
44	Measurement of energy and timing resolution of very highly pixellated LYSO crystal blocks with multiplexed SiPM readout for use in a small animal PET/MR insert. , 2013, , .		5
45	Development and evaluation of a LOR-based image reconstruction with 3D system response modeling for a PET insert with dual-layer offset crystal design. Physics in Medicine and Biology, 2013, 58, 8379-8399.	1.6	24
46	Performance evaluation of SensL SiPM arrays for high-resolution PET. , 2013, , .		7
47	Characterization of a handheld gamma camera for intraoperative use for sentinel lymph node biopsy. , 2013, , .		0
48	18F, 11C and 68Ga in small animal PET imaging. Nuklearmedizin - NuclearMedicine, 2013, 52, 250-261.	0.3	5
49	Use of systematic surface roughing to enhance the spatial resolution of the dual-ended readout of axially-oriented 100 mm long LYSO crystals. Physics in Medicine and Biology, 2012, 57, N501-N512.	1.6	4
50	Application of HDMI® cables as an MRI compatible single cable solution for Readout and power supply of SiPM based PET detectors. , 2012, , .		10
51	A MPPC based tool for timing and spatial resolution characterization of PET detectors. , 2012, , .		1
52	Estimation of NECR, scatter fraction, and sensitivity of a new MR compatible small animal PET insert based on Monte-Carlo simulations. , 2012, , .		0
53	Analytical modeling and implementation of detector response for fully 3D computer simulation and image reconstruction of an MRI compatible PET insert with a dual-layer offset crystal design. , 2012, , .		2
54	NEMA NU 4-2008 Comparison of Preclinical PET Imaging Systems. Journal of Nuclear Medicine, 2012, 53, 1300-1309.	2.8	191

#	Article	IF	CITATIONS
55	Evaluation of very highly pixellated crystal blocks with SiPM readout as candidates for PET/MR detectors in a small animal PET insert. , 2012, , .		7
56	Evaluation of High Density Pixellated Crystal Blocks With SiPM Readout as Candidates for PET/MR Detectors in a Small Animal PET Insert. IEEE Transactions on Nuclear Science, 2012, 59, 1791-1797.	1.2	28
57	Calibration of Dual-Ended Readout of Axially Oriented 100-mm-Long LYSO Crystals for Use in a Compact PET System. IEEE Transactions on Nuclear Science, 2012, 59, 561-567.	1.2	8
58	Five-year experience of quality control for a 3D LSO-based whole-body PET scanner: Results and considerations. Physica Medica, 2012, 28, 210-220.	0.4	12
59	Validation of a GATE Model of \$^{176}\$Lu Intrinsic Radioactivity in LSO PET Systems. IEEE Transactions on Nuclear Science, 2011, 58, 682-686.	1.2	20
60	Variations on the NEMA NU4-2008 testing procedures and effect on the performance measurement results. , 2011, , .		2
61	Evaluation of a 16:3 Signal Multiplexor to Acquire Signals From a SPM Array With Dual and Single Layer LYSO Crystal Blocks. IEEE Transactions on Nuclear Science, 2011, 58, 2175-2180.	1.2	25
62	Quantitative computed tomography in porcine lung injury with variable versus conventional ventilation: Recruitment and surfactant replacement*. Critical Care Medicine, 2011, 39, 1721-1730.	0.4	57
63	Observations on dual-ended readout of 100mm long LYSO crystals. Nuclear Instruments and Methods in Physics Research, Section A: Accelerators, Spectrometers, Detectors and Associated Equipment, 2011, 652, 275-279.	0.7	4
64	On the Significance of Defective Block Detectors in Clinical 18F-FDG PET/CT Imaging. Molecular Imaging and Biology, 2011, 13, 265-274.	1.3	6
65	Viability and proliferation potential of adipose-derived stem cells following labeling with a positron-emitting radiotracer. European Journal of Nuclear Medicine and Molecular Imaging, 2011, 38, 1323-1334.	3.3	35
66	Resolution of pulmonary edema with variable mechanical ventilation in a porcine model of acute lung injury. Canadian Journal of Anaesthesia, 2011, 58, 740-750.	0.7	25
67	Bone microarchitecture assessed by TBS predicts osteoporotic fractures independent of bone density: The manitoba study. Journal of Bone and Mineral Research, 2011, 26, 2762-2769.	3.1	486
68	Improvement in spatial resolution of dual-ended readout of 100 mm long LYSO Crystals through use of systematic crystal surface roughing. , 2011, , .		1
69	Evaluation of high density pixilated crystal blocks with SiPM readout as candidates for PET/MR detectors in a small animal PET insert. , 2011, , .		9
70	Simulation guided optimization of Dual Layer Offset detector design for use in small animal PET. , 2011, , .		7
71	Evaluation of the SensL SPMMatrix for use as a detector for PET and gamma camera applications. , 2011, , ,		1
72	A method for measuring the energy spectrum of coincidence events in positron emission tomography. Physics in Medicine and Biology, 2010, 55, 535-549.	1.6	8

ANDREW L GOERTZEN

#	Article	IF	CITATIONS
73	Validation of GATE simulations of the ¹⁷⁶ Lu intrinsic activity in LSO detectors. , 2009, , .		Ο
74	Coincidences originating from a single photon: An unrecognized and potentially significant source of scatter in small animal PET?. , 2009, , .		2
75	Practical Aspects of 18F-FDG PET When Receiving 18F-FDG from a Distant Supplier. Journal of Nuclear Medicine Technology, 2009, 37, 164-169.	0.4	30
76	Accelerated microPET Transmission Imaging. IEEE Transactions on Nuclear Science, 2008, 55, 2501-2507.	1.2	0
77	Improvement of the spatial resolution of the MicroPET R4 scanner by wobbling the bed. Medical Physics, 2008, 35, 1223-1231.	1.6	21
78	A comparison of methods to calculate the energy spectrum of a PET system operating in coincidence mode. , 2007, , .		0
79	Imaging of Weak-Source Distributions in LSO-Based Small-Animal PET Scanners. Journal of Nuclear Medicine, 2007, 48, 1692-1698.	2.8	45
80	Quantifying the effects of defective block detectors in a 3D whole body pet camera. , 2007, , .		2
81	Radiosynthesis of <i>cis</i> â€4â€[¹²⁴ 1]iodoâ€ <scp>L</scp> â€proline as a prototype prob for imaging anterograde axoplasmic transport systems using positron emission tomography (PET). Journal of Labelled Compounds and Radiopharmaceuticals, 2007, 50, 636-637.	e 0.5	0
82	Evaluation of the Spatial Resolution Improvement of the MicroPET R4 Scanner with a Wobbling Bed. , 2006, , .		1
83	On the Imaging of Very Weak Sources in an LSO Pet Scanner. , 2006, , .		4
84	First results from the high-resolution mouseSPECT annular scintillation camera. IEEE Transactions on Medical Imaging, 2005, 24, 863-867.	5.4	40
85	A method for determination of the timing stability of PET scanners. IEEE Transactions on Medical Imaging, 2005, 24, 1053-1057.	5.4	9
86	A comparison of x-ray detectors for mouse CT imaging. Physics in Medicine and Biology, 2004, 49, 5251-5265.	1.6	39
87	Effect of phantom voxelization in CT simulations. Medical Physics, 2002, 29, 492-498.	1.6	25
88	Simultaneous molecular and anatomical imaging of the mousein vivo. Physics in Medicine and Biology, 2002, 47, 4315-4328.	1.6	86